[CANCER RESEARCH 62, 4100–4108, July 15, 2002]

Transcript Map of the 3.7-Mb *D19S112–D19S246* Candidate Tumor Suppressor Region on the Long Arm of Chromosome 19[1]

Christian Hartmann, Loki Johnk, Gaspar Kitange, Yanhong Wu, Linda K. Ashworth, Robert B. Jenkins, and David N. Louis[2]

Molecular Neuro-Oncology Laboratory, Department of Pathology and Neurosurgical Service, Massachusetts General Hospital and Harvard Medical School, Boston, Massachusetts 02129 [C. H., L. J., D. N. L.]; Division of Laboratory Genetics, Mayo Clinic and Foundation, Rochester, Minnesota [G. K., Y. W., R. B. J.]; and Lawrence Livermore National Laboratory, Livermore, California and Department of Energy Joint Genome Institute, Walnut Creek, California [L. K. A.]

ABSTRACT

Allelic losses of the q13.3 region of chromosome 19 have been documented in malignant gliomas, neuroblastomas, and ovarian carcinomas, strongly suggesting the presence of a 19q13.3 tumor suppressor gene. Deletion mapping in tumors over the past decade has narrowed the candidate region considerably but has produced partially conflicting results, with some small candidate regions defined only by isolated tumors with deletions. Mutation and expression screening of genes from the most likely candidate regions has failed to identify the gene of interest, perhaps because of the conflicting deletion mapping data. The recently increased public availability of human genomic sequence, combined with improved bioinformatics capabilities, has now made it possible to map much larger candidate regions in considerable detail. We have manually generated a transcript map that spans most of the 19q13.3 tumor suppressor candidate region, from *D19S219* to *D19S246*, with a resolution and quality superior to that of computer-generated maps. These results are presented in the hope that an improved map of the candidate region will facilitate further widespread screening and eventual identification of the gene or genes deleted in human gliomas, neuroblastomas, and ovarian cancers.

INTRODUCTION

Allelic losses of the long arm of chromosome 19 in a variety of human malignancies strongly suggest that 19q harbors a tumor suppressor gene. Loss of 19q is found commonly in all three major types of diffuse human malignant gliomas (1–5) as well as in epithelial ovarian cancers and neuroblastomas (6–8). Indeed, this region is already of clinical importance, because 19q loss in combination with 1p loss is associated with a greater likelihood of chemosensitivity, more durable chemotherapeutic responses, and longer overall survival in patients with anaplastic oligodendrogliomas (9–11). There has, therefore, been considerable interest in identifying the putative tumor suppressor gene from this candidate region.

Deletion mapping studies of malignant gliomas have gradually narrowed the candidate region over the past decade (Fig. 1). A common region of loss in astrocytomas was initially found between 19q13.11 and 19q13.4 (12, 13) and was then reduced to a 9.5-Mb area between *D19S178* on 19q.13.2 and *D19S180* on 19q13.4 (14) and to a 4-Mb region on 19q13.3 between *APOC1* and *HRC* (15). Subsequently identified 1.4-Mb deletion areas between *D19S412* and *STD* (16) and between *D19S241E* and *D19S596* (17) defined a minimal common deletion region of 150 kb (17). Sequencing of this 150-kb candidate region revealed *GLTSCR1*, *EDH2*, *GLTSCR2*, and *SW*, but no mutations or expression abnormalities were found in these genes (18, 19). Recent deletion mapping in neuroblastomas has demonstrated a commonly deleted region between *D19S412* and *D19S606*, overlapping the larger glioma candidate regions but excluding the 150-kb glioma candidate region (7). On the other hand, one glioma has been reported with an interstitial loss of a 425-kb region between *D19S219* and *D19S112* at 19q13.3 (20), centromeric to the probable glioma/neuroblastoma locus. Conversely, epithelial ovarian cancer deletions apparently overlap more telomerically on 19q13.3, between *D19S246* and the *KLK* gene family (8). There is thus controversy in assigning the most likely location for the 19q tumor suppressor, with some candidate regions based only on a small number of deletions in genetically unstable tumors, and it remains possible that the region contains more than one tumor suppressor locus. These difficulties have thwarted identification of the gene, or genes, of interest.

Although traditional gene-hunting strategies required mapping a region of interest to a few hundred kilobases, the public availability of extensive draft sequences from the human genome and of computer bioinformatics programs has made it possible to map much larger candidate regions. This event has in turn raised the possibility that a larger transcript map could be probed more effectively for the 19q gene than smaller maps following more traditional approaches. Here we present a manually generated transcript map that spans most of the 19q13.3 tumor suppressor candidate regions, from *D19S219* to *D19S246*, with a resolution superior to that of currently available computer-based maps. The map covers a candidate region defined by many tumor breakpoints, reducing the likelihood that genomic instability in individual tumors could direct gene identification strategies to an incorrect locus. This large transcript map thus lays the groundwork for the prioritization of 19q tumor suppressor gene candidates and the determination of their involvement in these important human malignancies by further high-throughput screening studies.

MATERIALS AND METHODS

Physical Map. An approximately 3.7-Mb physical map spanning the region from *D19S112* to *D19S246* was generated using 28 BACs[3] and 19 cosmids/fosmids sequenced by LLNL (Table 1). Publicly available scaffolds GA_x2KMHMR58TM, GA_x2KMHMR58UK, GA_x2KMHMR58JG, GA_x2KMHMR58W5, GA_x2KMHMR58UK, GA_x2KMHMR592L, GA_x2KMHMR58HM, GA_x8WDQ41, GA_x8WDQ6N, GA_x8WDQ6T, and GA_x8WDQ7U from Celera (Celera Genomics, Rockville, MD) were then applied to control for sequence ordering and quality and also to fill gaps. Results from an earlier shotgun sequencing project of the minimal deletion region based on BAC 284K17 were also included (18). BAC and cosmid/fosmid order was also accomplished using the chromosome 19q arm metric physical map from LLNL.[4] Discrepancies were resolved within the human genome BAC clone map, based on shared restriction fragments from the Genome Sequence Center of Washington University School of Medicine, St. Louis.[5] Sequence assembly was accomplished with SeqMan II 5.0 (DNAstar, Madison, WI) and Staden-Package 2000.0.[6]

Identification of Genes, CpG Islands, and Promoter Regions. Genes were identified by two different strategies. Nucleotide similarity searches with

Received 3/1/02; accepted 5/9/02.

The costs of publication of this article were defrayed in part by the payment of page charges. This article must therefore be hereby marked *advertisement* in accordance with 18 U.S.C. Section 1734 solely to indicate this fact.

[1] Supported by NIH Grants CA69285 (to D. N. L.) and CA85799 (to R. B. J.).

[2] To whom requests for reprints should be addressed, at Molecular Neuro-Oncology Laboratory, CNY6, Massachusetts General Hospital, 149 Thirteenth Street, Charlestown, MA 02129. Phone: (617) 726-5510; Fax: (617) 726-5079; E-mail: louis@helix.mgh.harvard.edu.

[3] The abbreviations used are: BAC, bacteria artificial chromosome; LLNL, Lawrence Livermore National Laboratory; hEST, human expressed sequence tag.

[4] Internet address: http://greengenes.llnl.gov/genome-bin/loadmap?region = mq.

[5] Internet address: http://genome.wustl.edu/gsc/human/Mapping/index.shtml.

[6] Internet address: http://www.mrc-lmb.cam.ac.uk/pubseq/staden_home.html.

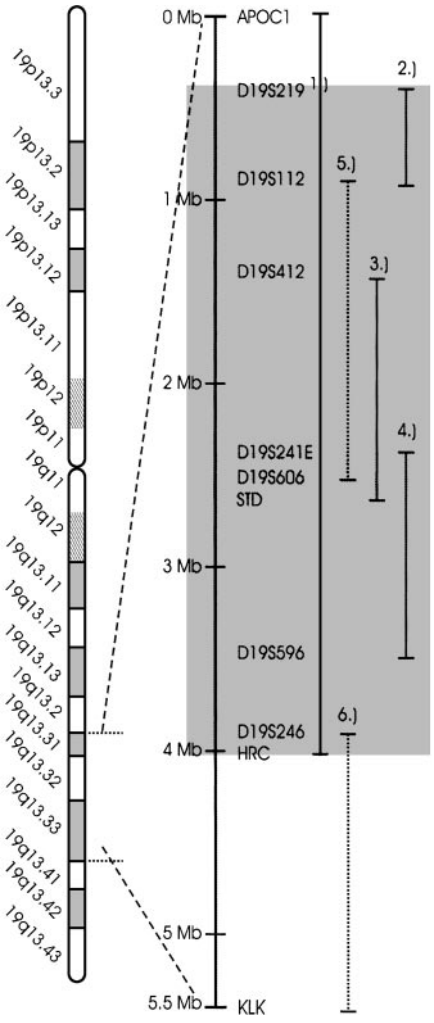

Fig. 1. Prior mapping studies demonstrating partially overlapping common deletion areas (between *D19S241E* and *STD*) on 19q13.3, spanning 5.5 Mb; *1*, Rubio *et al.* (15); *2*, Yong *et al.* (20); *3*, Rosenberg *et al.* (16); *4*, Smith *et al.* (17); *5*, Mora *et al.* (7) in neuroblastoma; *6*, Bicher *et al.* (8) in ovarian cancer.

BLAST 2.0 were performed using the nr (restricted to *Homo sapiens*), hEST, and mEST (parameters: expect = 0.0001, word size = 11, filters = low complexity and for nr also human repeats) databases. Database queries were executed locally and on National Center for Biotechnology Information Blast servers. Results were assessed manually to test the logical stringency of gene candidates, using criteria such as full-length completeness, multiple appearance of sequence motifs, and correct splicing sites. Genomic sequences were also analyzed by the gene prediction programs GrailEXP 2.0[7] and Genscan.[8] If only hESTs and predicted exons were available, results from both strategies were manually evaluated to test the importance of possible gene candidates. CpG islands were identified by GrailEXP, CpG Islands[9] and WebGene[10] and rejected if a distance of >7 kb separated the island from exon 1 of a gene candidate. The value of predicted CpG islands was further evaluated by overlapping the region with predicted promoter sites generated by the promoter prediction programs Neural Network Promoter Prediction,[11] Promoter 2.0 Prediction Server,[12] WWW Signal Scan,[13] and Transfac.[14]

[7] Internet address: http://grail.lsd.ornl.gov/grailexp.
[8] Internet address: http://genes.mit.edu/GENSCAN.html.
[9] Internet address: http://www.ebi.ac.uk/cpg.
[10] Internet address: http://www.itba.mi.cnr.it/cgi-bin/webgene/webgene_launcher.
[11] Internet address: http://www.fruitfly.org/seq_tools/promoter.html.
[12] Internet address: http://www.cbs.dtu.dk/services/promoter.
[13] Internet address: http://bimas.dcrt.nih.gov/molbio/signal.
[14] Internet address: http://transfac.gbf.de/TRANSFAC/index.html.

Further Characterization of Genes. Expression patterns were tested using SAGE,[15] with the mRNA sequence of each gene analyzed according to SAGE tags, to determine whether there was higher expression in normal brain than in glioma or higher expression in low-grade than in high-grade glioma. Possible functions of the gene products were determined by literature review and mRNA sequence analysis. To this end, the mRNA sequence was translated by Gene Runner 3.05 (Hastings Software, Hudson, NY) in all three possible reading frames, blasted against protein-nr, and analyzed for conserved protein motifs by RPS-blast using the Conserved Domain Database based on Pfam and Smart. Because genes that regulate key cellular functions, including tumor suppressor genes, are often highly conserved during evolution, the 107 genes were compared among different species using protein BLAST and by BLAST comparison of the genomic sequence against the mouse EST database.

RESULTS

Physical Map. Three sequence contigs were assembled that cover the entire 3.7-Mb region (Fig. 2): a centromeric contig of 1852 kb (Fig. 2*a*), a small middle contig of 108 kb (Fig. 2*b*), and a telomeric contig of 1791 kb (Fig. 2*c*). The size of the two remaining gaps is unknown, but each is likely to be <10 kb, given the few and small remaining sequences from the corresponding draft version BAC sequence files. Seven gaps of known size (average size, 8 kb) remain in the centromeric contig and 6 gaps in the telomeric contig, but it is unlikely that these gaps contain new genes; the surrounding regions contain no common gene characteristics (incomplete cDNA alignments, incomplete exons, or CpG islands), and the small size of the gaps would only allow single-exon genes. Comparison of publicly available sequences with the previously mapped 150-kb minimal deletion area (17) and with sequence material from an earlier shotgun sequencing project (18) revealed no significant differences. Most of the markers defining the margins of the common regions of overlap were identified on the three contigs; the microsatellite marker *D19S412* was found at position 1,067,000 in the centromeric contig, and the *STD* gene was identified near position 450,000 of the telomeric contig (Fig. 1, *number 3*; Ref. 16). The microsatellite marker *D19S241E* was seen at position 1,833,000 in the centromeric contig, *D19S596* at position 1,275,000 of the telomeric contig, and the 150-kb minimal deletion area aligned between positions 248,000 and 359,000 in the telomeric contig (Fig. 1, *number 4*; Ref. 17). The recently mapped common deletion region in neuroblastomas was found between position 1,067,000 (*D19S412*) of the centromeric contig and 42,000 (*D19S606*) of the telomeric contig (Fig. 1, *number 5*; Ref. 7). All three common regions of overlap span the middle contig and the two gaps of unknown size. The microsatellite marker *D19S219* was identified at position 51,000 of the centromeric contig, the marker *D19S112* at 437,000 on the same contig (20). Interestingly, when compared with the published data, the two markers *D19S246* (position 1,668,000 on the telomeric contig) and *HRC* (position 1,680,000 on the telomeric contig) were found in reverse order and much closer to each other (Fig. 1, *numbers 1* and *6*) than reported previously (8, 15).

Transcript Map. BLAST and gene prediction programs identified 107 possible genes in the three contigs, some with multiple copies and 85 (79%) with CpG islands close to exon 1. Fig. 2 presents the basic features of the map, and some gene details are given in Table 2. The following section highlights features of some of the genes on each of the three contigs.

Forty-three genes mapped to the centromeric contig, some of particular interest as candidate genes. Between *D19S219* and *D19S112* is the myotonic dystrophy region containing the *DMPK* and *DMWD* genes. Approximately 80 kb telomeric to *D19S112* lies the *NOVA2* gene en-

[15] Internet address: http://www.ncbi.nlm.nih.gov/SAGE.

Table 1 *List of all BACs, fosmids, and cosmids between D19S219 and D19S246 sequenced by LLNL in centromeric to telomeric order*

BAC[a]	GenBank	Contig
F13544	M77823	CC
F20720	AC006117	CC
R32889	AC006261	CC
BC77051	AC011480	CC
R28204	AC006132	CC
R34072	AC007191	CC
R26955	AC007774	CC
F18894	AC074212	CC
R26777	AC011530	CC
BC34685	AC008623	CC
F23842	AC006540	CC
R30477	AC011545	CC
BC282485	AC007785	CC
BC264576	AC006262	CC
BC82621	AC007193	CC
F22900	AC024584	CC
BC89981	AC011484	CC
R31455	AC011551	CC
BC267100	AC026776	CC
BC96400	AC008635	CC
BC86001	AC008622	CC
BC682294	AC008895	CC
BC831365	AC008755	CC
BC335879	AC008532	CC
R27648	AC010514	CC/MC
BC830112	AC008754	MC
BC388229	AC073548	MC/TC
BC894691	AC016589	TC
BC821616	AC010331	TC
F24003	AC008985	TC
R30005	AC010519	TC
BC782556	AC008745	TC
BC858854	AC024582	TC
BC815354	AC010330	TC
BC694629	AC010458	TC
BC324323	AC011466	TC
BC242886	AC008392	TC
R33773	AC020955	TC
F16353	AC011514	TC
R26730	AC011527	TC
BC255070	AC008403	TC
BC677569	AC008888	TC
R31763	AC009002	TC
BC808482	AC026803	TC
BC52308	AC008687	TC
BC679592	AC008891	TC

[a] BAC, LLNL BAC, PAC, fosmid or cosmid ID; GenBank, GenBank accession ID; Contig, location of the sequence; CC, centromeric contig; MC, middle contig; TC, telomeric contig.

coding an RNA-binding protein (21). The next telomeric gene, *PGLYRP*, has similarities with to the tumor necrosis family superfamily, whereas the newly identified gene *TGIF3* contains a HOX homeobox domain. The mRNA sequence *DKFZp434J0226* was seen at two locations on the same genomic DNA strain, enclosing the gene *RPL12*. The second copy of *DKFZp434J0226* exhibited no first exon. In both cases, the sequence is not translatable, but matching hESTs can be found; therefore, it remains unclear whether this is a processed pseudogene or whether noncoding RNA is the ultimate product. More than 900 kb centromeric to *D19S412*, the previously cloned and analyzed candidate gene *PPP5C* (22) appeared on the centromeric contig. The 7-exon putative tumor suppressor gene *Rho-GAP p190-A* (23, 24) was located 300 kb centromeric to the common deletion area. The 7-exon gene *KIAA1722* also maps to the same genomic sequence, suggesting that it is a larger splicing variant of *p190-A*. Although there are no significant differences in the translated amino acid sequence, the noncoding exons 6 and 7 differ greatly in size between the two transcripts. The p53 up-regulated modulator of apoptosis (*PUMA*)/Bcl2-binding component 3 (*bbc3*) gene and SUMO-1 activating factor (*SAE1*) genes were located 40 and 100 kb centromeric to *D19S241E*, respectively, and were covered by three common deletion regions.

Four genes were identified in the small middle contig. The centromeric/telomeric orientation of this contig was based on assembling multiple BACs, with BAC position determined by the LLNL BAC map. Although it was possible to assign *C5aR*, *C5L2*, and *KIAA0134* completely to the middle contig, positions 1 to 373 of *DKFZp547H236* were not identified in the sequence. Presumably, the first exon or exons of the gene are located within the gap between the middle and the telomeric contig, because the subsequent exon of DKFZp547H236 aligns very close to the telomeric border of the contig.

The telomeric contig contained 61 genes. Although most chromosomes have a gene density of 7–15 genes/Mb (chromosome 19, 20 genes/Mb; Ref. 25), the telomeric contig has nearly 41 genes/Mb. Within the minimal deletion area, no new genes were identified, aside from the already cloned and analyzed *GLTSCR1*, *EDH2*, *GLTSCR2*, and *SW* (18). Interestingly, two mRNA sequences, *FLJ00085* and *DKFZp434C031*, are splicing variants of *GLTSCR2*. Although *GLTSCR2* has an mRNA length of 1516 bp, *FLJ00085* has a length of 4186 bp, covering all exons and introns 6, 7, and 10 of *GLTSCR2*. Alternatively, the 1762-bp *DKFZp434C031* starts with exon 6 of *GLTSCR2*. Exons 5 and 8 of *DKFZp434C031* are longer than the corresponding exons 10 and 13 of *GLTSCR2*, and the last two exons of *DKFZp434C031* are not part of the *GLTSCR2* sequence. Only partial hESTs were found that align to these alternate sequences. Another 1468-bp sequence, which is 96% identical to *GLTSCR2*, was described as *P60*, coding for a protein that interacts with the herpes simplex virus 1 regulatory proteins ICP22 and ICP0 (26). No coding sequences were identified within 120 kb centromeric to the 150-kb minimal common deletion area. Only isolated hESTs and single predicted exons were seen, suggesting an absence of genes in this region. However, because of a 10-kb gap within this area, there is still the possibility of an unidentified gene. On the other hand, 9 kb telomeric to the minimal deletion area, a 496-bp putative single-exon gene was found with an open reading frame of 115 amino acids, showing homologies to the ribosomal protein *L23a*. Near the UniGene cluster Hs.104894, recently described as epididymal sperm binding protein (*ELSPBP1*; Ref. 27), the gene *CaBP5* was localized. However, there was no evidence for exons 4 to 6 of *CaBP3*, described as being on the opposite strand and sharing the reverse sequence of exons 1 to 3 of *CaBP5* (28).

The 10-exon gene *CARD8/KIAA0955* was found 400 kb telomeric to the 150-kb minimal common deletion area. The genes *NDPP1* and *DACAR* also align to the *CARD8* sequence; however, they cover only exon 3 to the beginning of exon 10. By assembling the corresponding UniGene cluster Hs.10031 and aligning the resulting consensus sequence, an additional 160-bp exon "0" was identified 6.2 kb upstream to exon 1. The UniGene cluster Hs.310472 (internal name *JAZ-1*) aligns to the genomic sequence near *CARD8* and contains a KRAB box in the translated protein, thereby identifying it as another member of the zinc finger family. Another promising candidate within the same region is the glutamate-rich WD repeat protein (*GRWD*), with 7 exons and a length of 2240 bp. The putative apoptosis-associated tyrosine kinase 2 (*AATK2*) gene was found close to *GRWD*. This gene was assembled based on the cDNA *KIAA1883*, UniGene cluster Hs.281328, other hESTs and GrailEXP-generated exon candidates and appears to code for a tyrosine kinase that is similar to *AATK* (or *AATYK*). The phosphoinositol 3-phosphate binding protein-1 (*PEPP1*) gene was found telomeric to *D19S596*. This gene, which contains a pleckstrin homology domain and codes for a signaling protein of unknown function, was initially described as being expressed only in melanocytes and melanoma cells (29). However, the SAGE tags were also found in different gliomas, indicating a higher expression in low-grade than high-grade tumors. The two apoptosis-regulating genes, *GADD34* and *BAX*, which are within close proximity to each other, were identified 130 and 220 kb telomeric to *D19S596*, respectively. Because early studies mapped the candidate gene *BAX* to 19q13.3, it was one of the first genes screened for mutations (30).

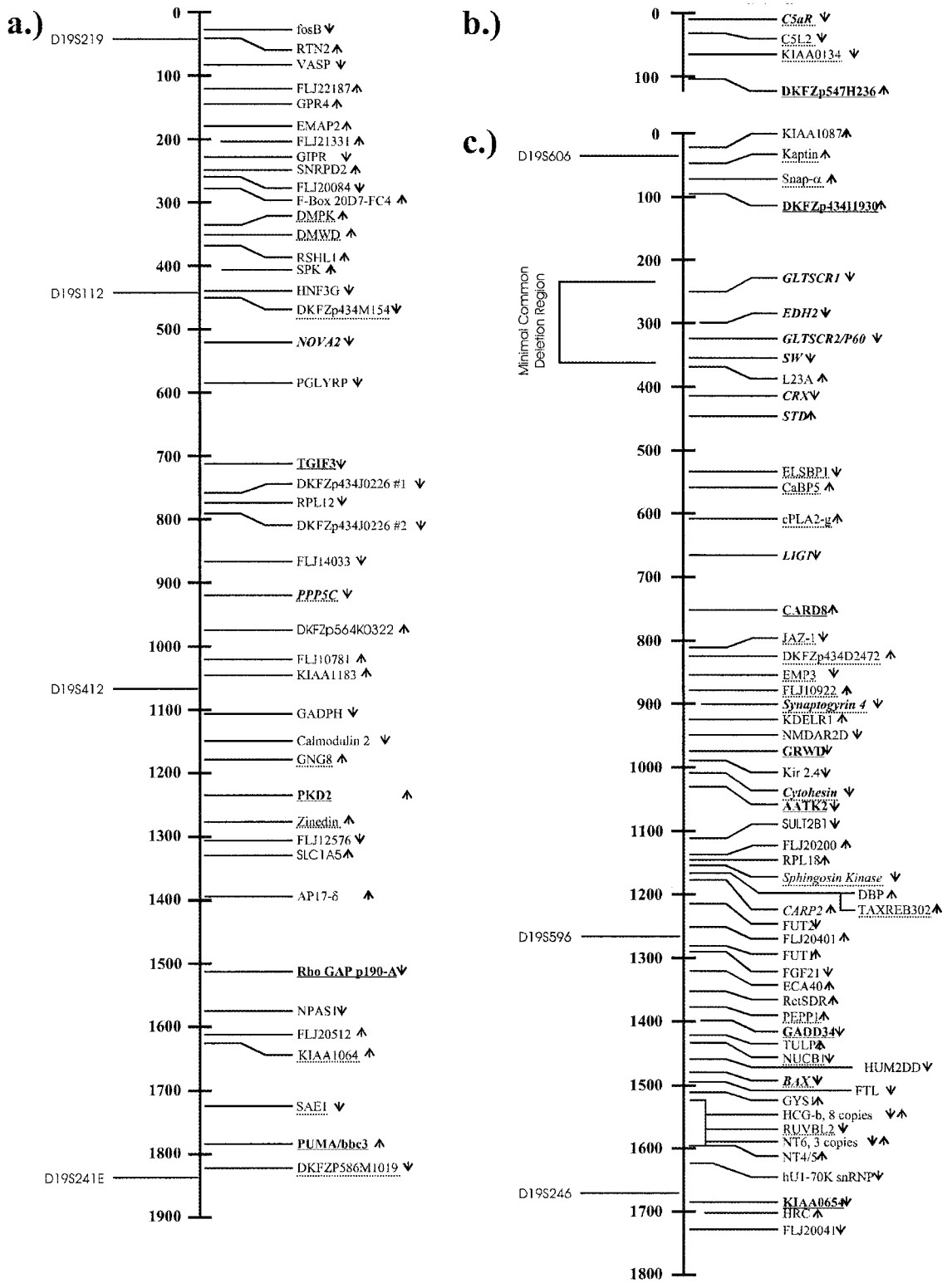

Fig. 2. Gene map between *D19S219* and *D19S246*, spanning 3.7 Mb. *a*, centromeric contig (CC, 1852 kb). *b*, middle contig (MC, 107 kb). *c*, telomeric contig (TC, 1791 kb). *Arrows* behind gene names, position of gene on the forward or reverse DNA strand; *italic* gene names, genes tested for mutation in earlier studies; *lines pointing* to a genomic spot, the central position of the corresponding gene. The minimal deletion region is based on Smith *et al.* (17).

An interesting cluster of genes was observed 100 kb centromeric to *D19S246*; 8 copies of *HCG-β* and 3 copies of *NT6* were present on both strands, falling within *RUVBL2* and *NT4/5*. The 4716-bp cDNA *KIAA0654* aligned with *D19S246* in the telomeric contig. *FLJ22319* (3886 bp) and *FLJ13788* (1616 bp) are two other cDNAs that are identical to *KIAA0654*. The 1440-bp mRNA of *Liprin-alpha 3* aligns to position 2586-4110 of the *KIAA0654* sequence, indicating splicing variants of this gene. Whereas earlier mapping studies placed the *HRC* gene centromeric to *D19S246* (8, 15), the genomic DNA sequence revealed *HRC* to be 20 kb telomeric to the microsatellite marker.

Table 2 *List of all genes between D19S219 and D19S246*

Gene	GenBank	Len[a]	Ex	CpG	Protein motifs	Functional suggestion	Comment
AATK2	Hs.281328	2549 (?)	18	+	TyrKc, pkinase, S_TKc	Apoptosis	High similarities with apoptosis-associated tyrosine kinase (AATK)
AP17-d	NM_021575	667	4	+	Clat_adaptor_s, Adap_comp_sub	Clathrin adaptor complex	
BAX	NM_004324	657	6	+	Bcl-2, BCL	Apoptosis	
C5aR	NM_001736	2328	1	−	7tm_1	G protein-coupled receptor	Inflammatory response
C5L2	NM_018485	1287	2	−	7tm_1	G protein-coupled receptor	Inflammatory response
CaBP5	AF169159	1226	6	−	Efhand, Efh	Calcium binding protein	CaBP3 not detectable
Calmodulin 2	BC005137	2190	7	+	Efhand, Efh, EH	Calmodulin gene	
CARD8	NM_014959	5059	10	−	CARD	Apoptosis, Caspase activation	Identical with *KIAA0955*
CARP2	AF067662	1488	9	−	carb_anhydrase	Carbonic anhydrase	
CRX	NM_000554	900	3	−	Homeobox, HOX	Homebox gene	Cone-rod dystrophy gene
Cytohesin	U70728	1361	9	+	Sec7, PH	Signaling protein	
DBP	U06936	1403	4	−	BRLZ	Albumin D-box binding protein	Partly same sequence like *TAXREB302*
DKFZp434D2472	AL122083	1907	7	−			
DKFZp434I1930	AL136846	2988	13	−	myb_DNA-binding, SANT	Transcriptional factor	
DKFZp434J0226	AL137376	1637	5	−			2 copies, not translatable
DKFZp434M154	BC005834	1971	1	+	zf-C3HC4	Zinc finger protein	
DKFZp547H236	AL359938	2404	14	(+)	Homeobox, HOX	Homebox gene	Mouse *meis 3* gene, potential oncogene
DKFZp564K0322	AL136609	2775	1	+			Similarities with paraneoplastic neuronal antigen Ma1
DKFZp586M1019	NM_015603	2026	12	+			
DMPK	NM_004409	3407	15	+	S_TKc, TyrKc, S_TK_X, ERM	Protein kinase	Dystrophia myotonica-protein kinase
DMWD	XM_027569	2893	4	+	WD40		Dystrophia myotonica-containing WD repeat
ECA40	U62739	1509	10	+	aminotran_4	Branched-chain amino acid aminotransferase	
EDH2	XM_009124	2175	5	+	EH		Similarities with hepatocellular carcinoma-associated protein HCA10
ELSBP1	NM_022142	1025	8	−	FN2	Fibronectin related	
EMAP2	NM_012155	2269	19	+	WD	Microtubule-associated	
EMP3	NM_001425	817	5	+	PMP22_Claudin	Myelin organisation	
F-box 20D7-FC4	XM_027578	1533	1	+	F-box		
FGF21	NM_019113	630	3	+	FGF	Part of acidic and basic fibroblast growth factor family	
FLJ10781	XM_009126	2713	2	+			
FLJ10922	NM_018273	2849	6	+			
FLJ12576	AK022638	2748	3	+			
FLJ14033	NM_022462	2595	15	−	PAS, PAC		Similar to hypoxia inducible factor 3 α
FLJ20041	AK000048	3810	23	+		Calcium channel	Similarities with LTRPC5, MLSN1, and TPR protein
FLJ20084	NM_017659	1574	8	+			Similarities with glutaminyl-peptide cyclotransferase
FLJ20200	NM_017708	1950	5	+			
FLJ20401	NM_017805	1457	5	+	DIL	Myosin related	
FLJ20512	AK000519	696	3	+			
FLJ21331	AK024984	2031	1	+			Alu warning after Blast-p
FLJ22187	NM_025136	1584	2	+			
fosB	NM_006732	3775	4	+		Oncogene	
FTL	NM_000146	723	4	+	ferritin	Ferritin, light polypeptide	
FUT1	NM_000148	3373	2	+	Glyco_transf_11	Fucosyltransferase 1 α(1,2)	
FUT2	NM_000511	1041	2	+	Glyco_transf_11	Fucosyltransferase	
GADD34	XM_009097	2349	3	+		Apoptosis	
GADPH	AF261085	1311	1	−	gpdh, gpdh_C	Glyceraldehyde-3-phosphate dehydrogenase	
GIPR	NM_000164	2025	14	−	7tm_2, HormR, HRM		Gastric inhibitory polypeptide receptor
GLTSCR1	XM_009125	5699	10	+			Similarities with collagen α 1(III) precursor
GLTSCR2	NM_015710	1516	13	+			Spliced exon variant between exon 6 and 7, identical with P60, interacting with HSV 1 early proteins
GNG8	NM_033258	213	2	−	GGL, g-gamma	G-protein gamma 8 subunit	
GPR4	NM_005282	2696	1	+	7tm_1	G protein-coupled receptor	Coagulation regulation
GRWD	AF337808	2240	7	+	WD40	Glutamate rich WD repeat protein	Similarities with retinoblastoma-binding protein 4/p48/CAF-1
GYS1	XM_009091	2886	13	+	Glycos_transf_1	Glycogen synthase 1	
HCG-β	NM_000737	539	3	(+)	GHB, Cys_knot	Chorionic gonadotropin, β polypeptide	8 copies, discrete differences in their sequence
HNF3G	XM_012811	1053	1	+	Fork_head, FH	Transcription factor	Hepatocyte nuclear factor 3 γ
HRC	XM_008915	2365	6	+			
hU1-70K snRNP	X06815	1672	11	+	rrm	hU1-70K small nuclear RNP protein	
HUM2DD	XM_009094	1005	7	+	GFO_IDH_MocA	Dimeric dihydrodiol dehydrogenase	

Table 2 *Continued*

Gene	GenBank	Len[a]	Ex	CpG	Protein motifs	Functional suggestion	Comment
JAZ-1	Hs.310472	1320 (?)	7	+	KRAB-box	Zinc finger gene	
Kaptin	NM_007059	1641	12	+		Actin-associated protein	
KDELR1	NM_006801	1086	5	+	ER_lumen_recept	Endoplasmic reticulum	
KIAA0134	NM_014681	4345	13	+	DEXDc, DEAD, SRP54, HELICc	Protein retention receptor 1 DEAD-like RNA helicases superfamily	
KIAA0654	AB014554	4716	27	+	SAM, ERM, Myosin_tail	Ezrin/radixin/moesin and tyrosine kinase motif	NF2 homologue?
KIAA1064	AB028987	5265	10	−	zf-CCCH	Zinc finger DNA-binding	
KIAA1087	AB029010	4282	10	−/−	Na_Ca_Ex, Calx_beta	Sodium/calcium exchanger protein	
KIAA1183	AB033009	2752	1	+			
Kir2.4	AF181988	5778	1	−	IRK	Inwardly rectifying potassium channel	
L23a	U43701	546	1	−	Ribosomal_L23	Ribosomal protein	
LIG1	NM_000234	3083	28	−	DNA_ligase, ligase	DNA ligase 1	
NMDAR2D	U77783	4299	13	+	PBPb, lig_chan, PBPe, SBP_bac_3, ANF_receptor	*N*-Methyl-D-aspartate receptor 2D subunit precursor	
NOVA2	XM_009129	1857	4	+	KH-domain		
NPAS1	AB054002	2065	11	+	HLA, PAS	Neuronal PAS domain protein 1	
NT4	M86528	1404	1	(+)	NGF	Nerve growth factor family	
NT5	XM_012904	633	1	(+)	NGF	Nerve growth factor family	5 copies, one is part of NT4, 4 are untranslatable pseudo genes
NT6	S41522	1143	1	(+)	NGF	Nerve growth factor family	2 translatable copies, 1 with an incomplete NGF motif, 2 pseudo genes
NUCB1	NM_006184	1654	13	+		DNA-binding protein	nucleobindin 1
PEPP1	XM_009098	3057	23	+	PH	Signaling protein	Phosphoinositol 3-phosphate binding protein
PGLYRP	XM_009130	690	3	−	Ami_2	Peptidoglycan recognition protein	Similar to TNF superfamily member 3
PKD2	AF309082	2900	17	+	C1, S_TKc, pkinase, TyrKc	Serine/threonine protein kinases	
PLA2G4C	AF065214	2472	17	+	PLAc, PAL2_B, UPF0028, ThiF_family	Group of cytosolic phospholipases	2 variants of exon 7
PPP5C	BC001970	2075	13	+	TPR, PP2Ac, STphosphatase	Protein phosphatase 5, catalytic subunit	
PUMA/bbc3	AF354654	1829	4	+	BH3	p53 apoptosis mediator	Bcl-2 binding component 3
RetSDR	NM_016246	1123	10	−	adh_shor,adh_short_C2	Retinal short-chain dehydrogenase/reductase	
RhoGAPp190-A	AF159851	4545	7	−	RAS, RAB, FF, RhoGAP	GTPase	Functionally a TSG, *KIAA1722* is a larger splicing variant
RPL12	XM_011829	608	1	−	Ribosomal_L11	Ribosomal protein	
RPL18	NM_000979	630	6	+	Ribosomal_L18e	Ribosomal protein	
RSHL1	NM_030785	2478	6	+			Ciliary function
RTN2	NM_005619	2190	11	+	Reticulon	ER organisation	
RUVBL2	XM_009417	1488	15	+	AAA	DnaB-like helicase	RuvB (*E. coli* homologue)-like 2
SAE1	BC000344	2076	9	+	ThiF_family	Ubiquitin complex	SUMO-1 activating enzyme subunit 1
SLC1A5	XM_012795	2844	8	+	SDF	Neutral amino acid transporter	Solute carrier family 1 member 5
Snap-a	U39412	1279	12	+		*N*-Ethylmaleimide-sensitive factor attachment protein	
SNRPD2	NM_004597	479	3		Sm	Pre-mRNA splicing	Small nuclear ribonucleoprotein D2
Sphingosin Kinase type 2	AF245447	23800	5	+	DAGKc	Protein kinase C activator	
SPK	XM_017129	2050	14	+			Symplekin Huntington interacting protein 1
STD	U08024	1780	6	−	Sulfotransfer	Dehydroepiandrosterone sulfotransferase	
SULT2B1	U92315	1228	7	+	Sulfotransfer	Hydroxysteroid sulfotransferase	
SW	AF015283	754	6	+		Selenoprotein W	
Synaptogyrin 4	NM_012451	872	4	+		Synaptogyrin gene family	
TAXREB302	D28468	1391	3	−	BRLZ	DNA-binding protein	Partly sequence like DBP
TGIF3	AF179900	608	2	−	HOX	Homebox gene	Similar to TGF-β induced transcription factor 2
TULP2	NM_003323	1733	13	+	Tub	Tubby-like protein 2	Involved in photoreceptor development
VASP	XM_009141	2176	13	+	WH1		Vasodilator-stimulated phosphoprotein
Zinedin	XM_009035	3156	18	+	WD40	Calmodulin-binding protein	

[a] Len, coding sequence length in base pairs; Ex, number of exons.

DISCUSSION

On the basis of the draft version of the Human Genome Project, publicly available genomic sequences that cover the common deletion regions between *D19S219* and *D19S246* were assembled into three contigs and were annotated for genes. Despite success in assembling these large contigs, some gaps remain. Presumably, the two gaps of unknown size are highly repetitive and cannot be sequenced. The 13 gaps (averaging 8 kb in size) in the centromeric contig and telomeric contig sequences are in regions not yet finished by the Joint Genome

Institute but are covered by publicly available Celera material. These data were of high enough quality to estimate the size of the remaining gaps, using algorithms provided by the company.

The draft results of the Human Genome Project estimated the number of genes at 30,000–45,000 (25, 31); however, >95,000 UniGene clusters are listed in the database. One explanation for this discrepancy is the presence of splicing variants, resulting in multiple UniGene clusters for one gene. In support of this hypothesis, many possible variants were identified within the annotated 19q13.3 region, and these variants often represented already characterized genes. Evaluation of splicing variants is relatively simple in cases such as *KIAA1722/Rho GAP p190-A*, *DKFZp547H236/human Meis3*, or *KIAA0654/Lin-7b*, because extant hEST material covers all relevant genomic areas, making it easier to verify that these are splicing variants. On the other hand, for genes such as *GLTSCR2*, for which *FLJ00085* and *DKFZp434C031* illustrate two alternate splicing variants (that include intronic areas of *GLTSCR2*), no matching hESTs can be identified. Such splicing variants may have low levels of expression, perhaps limited to specific tissues, or there could be general problems related to single-clone-for-single-gene cDNA sequences. Because of the nature of these cDNAs, the mRNA source may be premature and not completely spliced (32, 33). Aligning hESTs from the corresponding UniGene cluster with genomic DNA provides another method to test for possible splicing variants. For instance, using this approach, an additional 160-bp *CARD8* exon and a longer (43-bp) variant of *PLA2G4C* exon 15 were found.

New computer-based strategies thus make it possible to extend the candidate region dramatically, with a higher resolution, and with the identification of multiple putative variant forms. Functional classification, based on *in silico* comparison of the translated amino acid sequence with well-characterized proteins and known protein domains, predicted new genes involved in apoptosis (*CARD8*, *GRWD*, and *AATK2*), cell adhesion (*KIAA0654*), developmental regulation (*DKFZp547H236*), or transcriptional control (*DKFZp434I1930*, *DKFZp434M154*, and *JAZ-1*). Although such an approach can be helpful in reducing the number of candidate genes, it is important to recall that some known tumor suppressors did not, when initially identified, fit into an expected category of tumor-related genes. One such gene was the *NF2* gene, which encodes a moezin-, ezrin-, radixin-like protein (34). Additionally, many genes based on single-clone-for-single-gene methods did not contain any known protein domain or show similarities with characterized genes (*e.g.*, *DKFZp564M1019*, *FLJ10922*, and *KIAA1183*). The putative function of candidate genes is therefore helpful when relationships can be identified with known tumor-related genes, but negative results clearly do not exclude such genes as candidates.

We also examined expression patterns using the UniGene and SAGE databases. Although the evaluation of clustered hESTs from UniGene gives clear information concerning nervous system expression, different potential expression profiles of mutated tumor suppressor genes complicate interpretation of quantitative SAGE-based expression data from brain tumors. For instance, transcriptional levels can be reduced to zero in the presence of deletions, decreased mRNA stability, or mutations affecting the regulation of transcription. Expression can be reduced to 50% with a loss of one allele, whereas the transcriptional level of the remaining mutated allele is not affected or even elevated. For instance, an incorrectly folded protein may be proteolyzed faster, raising transcriptional activity via a positive feedback mechanism. Different expression patterns can result from distinct alterations in a single tumor suppressor gene, depending on type and location of the mutation (*e.g.*, *TP53*). Moreover, SAGE-based expression data are limited by the number of available libraries, the lack of tumor genotyping, and tissue heterogeneity of normal brain libraries. Custom cDNA microarrays could eliminate these SAGE-based problems and would be a logical next step in using expression data to evaluate tumor suppressor gene candidates in large chromosomal areas.

In the large candidate region, a number of genes involved in apoptosis, cell adhesion, developmental regulation, and cell cycle control are promising candidates. *TGIF3* (TALE homeobox TG-interacting factor 3), between *D19S219* and *D19S412*, is a new and highly conserved member of the TGIF protein family. Although the 1562-bp *TGIF* (18p11.3) and the 1647-bp *TGIF2* (20q11.2-12) have 3 exons, *TGIF3* has a cDNA length of 608 bp and presumably only 2 exons. TGIF homeodomain transcription factors contribute to Hox-mediated developmental programs (35), and up-regulation of *TGIF2* occurs in ovarian cancer cell lines (36). Because of the major cDNA sequence similarities to *TGIF*, SAGE could not determine an expression pattern for *TGIF3*; both genes contain the same sequence for the SAGE tags. Falling between *D19S412* and *D19S241E*, the conserved protein kinase D2 (*PKD2*) gene is covered by three common deletion regions and is widely expressed in many tissues, particularly in highly proliferative organs. Although PKD/PKCμ can be cleaved by caspase 3, thereby sensitizing cells to the cytotoxic effects of various genotoxic agents (37), the highly similar *PKD2* gene does not contain the cleavage site. Therefore, *PKD2* may serve a different function in apoptosis (38).

The highly conserved, putative tumor suppressor gene *Rho-GAP p190-A* maps more centromeric than initially reported (23). Functionally, p190-A can suppress ras-induced malignancy, and p190-A antisense RNA facilitates malignant transformation (39). However, SAGE expression data showed a highly variable distribution in the available glioma libraries. The nearby *PUMA*, or *bbc3*, gene is closer to *D19S241E*. This gene, which has a highly similar mouse homologue, has two p53-binding sites in its promoter and when expressed, results in extremely rapid apoptosis by binding to Bcl-2 and Bcl-X_L (40, 41). SAGE tags were unfortunately only available for four glioblastoma libraries, but in all cases these glioblastomas had low expression levels when compared with other tumors. Another candidate is *DKFZp547H236*, which is highly homologous to the mouse *TALE homeoprotein Meis3*. Interestingly, the highly similar family member *Meis1* was isolated as a common site of viral integration in a mouse model of acute myeloid leukemia (42). Overexpression of this gene, along with the presence of Hoxa9, induced acute myeloid leukemia, suggesting an oncogenic function (43). SAGE data show two groups of expression for this gene and illustrate the utility of the available SAGE information, normal brain and low-grade glioma libraries with high levels of expression *versus* glioblastomas having 20–50% comparative expression levels.

The cDNA *DKFZp434I1930* mapped centromeric to the 150-kb small deletion region, containing a Myb-like DNA-binding domain that was found with RPS-BLAST. Neither brain-derived ESTs nor useful SAGE tags were available, but its location and putative function make it a an attractive candidate, along with *CARD8*, which maps between *STD* and *D19S596*. Two recent binding studies showed partially contradictory results for the protein that harbors a CARD domain. In the first study, the protein was named tumor-up-regulated CARD-containing antagonist of caspase nine (TUCAN). It was found that TUCAN interferes with binding of Apaf1 to procaspase-9 and suppresses caspase activation induced by the Apaf1 activator, cytochrome *c*, thereby suggesting more an oncogenic function (44). The authors of the second study named the protein CARDINAL and found no interaction with procaspase-9 or other caspases. Their results indicate a negative regulation of the nuclear factor-κB pathway in a proinflammatory context (45). SAGE data indicated a lower expression level in high-grade, compared with low-grade, gliomas. Interest-

ingly, a comparison of mRNA and protein sequence to other species yielded no similarities.

The *GRWD* gene is another candidate gene found in this region. pBLASTing the protein sequence of this gene indicated a high level of conservation: *Mus musculus*, *Drosophila melanogaster*, *Caenorhabditis elegans*, *Saccharomyces cerevisiae*, *S. pombe*, *Arabidopsis thaliana*, and *Gallus gallus* all express highly analogous proteins. The same BLAST applied to human sequence yielded similarities to the human retinoblastoma-binding protein 4/p48 (G_1-S transition control protein-binding protein IEF-8502), a protein that negatively regulates ras in yeast (46). Furthermore, the conserved protein domain WD40 (repeated three times in the sequence) is found in many genes involved in apoptosis, transcriptional regulation, and cell cycle control, such as *APAF-1*, *TAFII-100*, and *CDC4*. The corresponding SAGE tag for *GRWD* can be found in multiple glioma libraries, but the differences in expression do not reveal any significant pattern. The putative apoptosis-associated tyrosine kinase 2 (*AATK2*) gene (*KIAA1883*) was found close to *GRWD* and contains a serine/threonine protein kinase domain. The highly similar *AATK* (or *AATYK*) gene on chromosome 17q25.3 is expressed during growth arrest and apoptosis of myeloid cells (47) and induces and promotes neuronal differentiation (48). Interestingly, *AATK2* specific SAGE tags were found in five normal brain libraries and only in one pilocytic astrocytoma. No high-grade glioma library contained a tag, indicating no expression of this gene in malignant gliomas. Ten hESTs derived from brain, fetal brain, kidney, and colon libraries indicated neuronal expression, which was similar to proteins from different species.

The 4716-bp *cDNA KIAA0654* overlaps directly with *D19S246*. The resulting protein contains both an ezrin/radixin/moesin motif, implying similarities with the tumor suppressor gene *NF2*, and a tyrosine kinase motif. *FLJ22319* (3886 bp), *FLJ13788* (1616 bp), and *Liprin-alpha 3* (mRNA length of 1440 bp) all align to the *KIAA0654* sequence, indicating splicing variants of this gene. The putative splicing variant *Liprin-alpha 3* lacks the ezrin/radixin/moesin domain. The Liprin family has been described as transmembrane protein-tyrosine phosphatases, involved in regulation of cell-matrix interactions and having similarities to the *APC* tumor suppressor gene (49). Interestingly, SAGE data revealed two groups of glioblastomas, differing in expression by a factor of 3 to 4.

This list of genes spans most of the common deletion regions mapped to 19q13.3 and thereby sets the stage for mutation screening as well as evaluations for other mechanisms of gene inactivation. One such possible mechanism relates to the remarkable number of CpG islands on chromosome 19. Most chromosomes have 5–15 islands/Mb (average, 10.5 islands/Mb); however, chromosomes 16, 17, and 22 have 19–22 islands/Mb. Strikingly, chromosome 19 is an extreme outlier, with 43 islands/Mb (25). This can be only partially explained by the high density of genes on chromosome 19, because the CpG islands/gene ratio still separates chromosome 19 from all others (average, 1.05 CpGs/gene; chromosome 19, 2.25 CpGs/gene). The remarkable density of CpG islands increases the attractiveness of the hypothesis that CpG hypermethylation might be a primary mechanism of silencing a 19q tumor suppressor gene. Curiously, in the oligodendroglioma subtype of malignant glioma, allelic loss typically affects large portions of the long arm of 19q, rather than the smaller, interstitial deletions described above for astrocytic malignant gliomas (16). At least 27 genes with tumor-related functions map between *D19S219* and *D19S246*, raising the possibility that allelic losses of a large portion of 19q might be related to either combined silencing of multiple genes by hypermethylation or haploinsufficiency for a combination of these genes (50). Methods to evaluate these possibilities, however, lag behind the well-defined approaches to mutation screening. Therefore, although the results of the Human Genome Project have been exceedingly helpful in mapping tumor-related regions and in identifying candidate genes, similar advances are necessary to facilitate the next step of evaluating such genes on a large scale. In this light, the present detailed map is reported in the hope that it will lay the foundations for additional physical mapping and the eventual identification of the gene that is lost so commonly in human gliomas, neuroblastomas, and ovarian cancers.

REFERENCES

1. von Deimling, A., Bender, B., Jahnke, R., Waha, A., Kraus, J., Albrecht, S., Wellenreuther, R., Fassbender, F., Nagel, J., Menon, A. G., *et al.* Loci associated with malignant progression in astrocytomas: a candidate on chromosome 19q. Cancer Res., *54:* 1397–1401, 1994.
2. Reifenberger, J., Reifenberger, G., Liu, L., James, C. D., Wechsler, W., and Collins, V. P. Molecular genetic analysis of oligodendroglial tumors shows preferential allelic deletions on 19q and 1p. Am. J. Pathol., *145:* 1175–1190, 1994.
3. Kraus, J. A., Koopmann, J., Kaskel, P., Maintz, D., Brandner, S., Schramm, J., Louis, D. N., Wiestler, O. D., and von Deimling, A. Shared allelic losses on chromosomes 1p and 19q suggest a common origin of oligodendroglioma and oligoastrocytoma. J. Neuropathol. Exp. Neurol., *54:* 91–95, 1995.
4. Bello, M. J., Leone, P. E., Vaquero, J., de Campos, J. M., Kusak, M. E., Sarasa, J. L., Pestana, A., and Rey, J. A. Allelic loss at 1p and 19q frequently occurs in association and may represent early oncogenic events in oligodendroglial tumors. Int. J. Cancer, *64:* 207–210, 1995.
5. Nakamura, M., Yang, F., Fujisawa, H., Yonekawa, Y., Kleihues, P., and Ohgaki, H. Loss of heterozygosity on chromosome 19 in secondary glioblastomas. J. Neuropathol. Exp. Neurol., *59:* 539–543, 2000.
6. Amfo, K., Neyns, B., Teugels, E., Lissens, W., Bourgain, C., De Sutter, P., Vandamme, B., Vamos, E., and De Greve, J. Frequent deletion of chromosome 19 and a rare rearrangement of 19p13.3 involving the insulin receptor gene in human ovarian cancer. Oncogene, *11:* 351–358, 1995.
7. Mora, J., Cheung, N. K., Chen, L., Qin, J., and Gerald, W. Loss of heterozygosity at 19q13.3 is associated with locally aggressive neuroblastoma. Clin. Cancer Res., *7:* 1358–1361, 2001.
8. Bicher, A., Ault, K., Kimmelman, A., Gershenson, D., Reed, E., and Liang, B. Loss of heterozygosity in human ovarian cancer on chromosome 19q. Gynecol. Oncol., *66:* 36–40, 1997.
9. Cairncross, J. G., Ueki, K., Zlatescu, M. C., Lisle, D. K., Finkelstein, D. M., Hammond, R. R., Silver, J. S., Stark, P. C., MacDonald, D. R., Ino, Y., Ramsay, D. A., and Louis, D. N. Specific genetic predictors of chemotherapeutic response and survival in patients with anaplastic oligodendrogliomas. J. Natl. Cancer Inst., *90:* 1473–1479, 1998.
10. Smith, J. S., Perry, A., Borell, T. J., Lee, H. K., O'Fallon, J., Hosek, S. M., Kimmel, D., Yates, A., Burger, P. C., Scheithauer, B. W., and Jenkins, R. B. Alterations of chromosome arms 1p and 19q as predictors of survival in oligodendrogliomas, astrocytomas, and mixed oligoastrocytomas. J. Clin. Oncol., *18:* 636–645, 2000.
11. Ino, Y., Betensky, R. A., Zlatescu, M. C., Sasaki, H., Macdonald, D. R., Stemmer-Rachamimov, A. O., Ramsay, D. A., Cairncross, J. G., and Louis, D. N. Molecular subtypes of anaplastic oligodendroglioma: implications for patient management at diagnosis. Clin. Cancer Res., *7:* 839–845, 2001.
12. von Deimling, A., Louis, D. N., von Ammon, K., Petersen, I., Wiestler, O. D., and Seizinger, B. R. Evidence for a tumor suppressor gene on chromosome 19q associated with human astrocytomas, oligodendrogliomas, and mixed gliomas. Cancer Res., *52:* 4277–4279, 1992.
13. Ransom, D. T., Ritland, S. R., Kimmel, D. W., Moertel, C. A., Dahl, R. J., Scheithauer, B. W., Kelly, P. J., and Jenkins, R. B. Cytogenetic and loss of heterozygosity studies in ependymomas, pilocytic astrocytomas, and oligodendrogliomas. Genes Chromosomes Cancer, *5:* 348–356, 1992.
14. von Deimling, A., Nagel, J., Bender, B., Lenartz, D., Schramm, J., Louis, D. N., and Wiestler, O. D. Deletion mapping of chromosome 19 in human gliomas. Int. J. Cancer, *57:* 676–680, 1994.
15. Rubio, M. P., Correa, K. M., Ueki, K., Mohrenweiser, H. W., Gusella, J. F., von Deimling, A., and Louis, D. N. The putative glioma tumor suppressor gene on chromosome 19q maps between *APOC2* and *HRC*. Cancer Res., *54:* 4760–4763, 1994.
16. Rosenberg, J. E., Lisle, D. K., Burwick, J. A., Ueki, K., von Deimling, A., Mohrenweiser, H. W., and Louis, D. N. Refined deletion mapping of the chromosome 19q glioma tumor suppressor gene to the *D19S412–STD* interval. Oncogene, *13:* 2483–2485, 1996.
17. Smith, J. S., Tachibana, I., Lee, H. K., Qian, J., Pohl, U., Mohrenweiser, H. W., Borell, T. J., Hosek, S. M., Soderberg, C. L., von Deimling, A., Perry, A., Scheithauer, B. W., Louis, D. N., and Jenkins, R. B. Mapping of the chromosome 19q-arm glioma tumor suppressor gene using fluorescence *in situ* hybridization and novel microsatellite markers. Genes Chromosomes Cancer, *29:* 16–25, 2000.
18. Smith, J. S., Tachibana, I., Pohl, U., Lee, H. K., Thanarajasingam, U., Portier, B. P., Ueki, K., Ramaswamy, S., Billings, S. J., Mohrenweiser, H. W., Louis, D. N., and Jenkins, R. B. A transcript map of the chromosome 19q-arm glioma tumor suppressor region. Genomics, *64:* 44–50, 2000.
19. Pohl, U., Smith, J. S., Tachibana, I., Ueki, K., Lee, H. K., Ramaswamy, S., Wu, Q., Mohrenweiser, H. W., Jenkins, R. B., and Louis, D. N. EHD2, EHD3, and EHD4 encode novel members of a highly conserved family of EH domain-containing proteins. Genomics, *63:* 255–262, 2000.

20. Yong, W. H., Chou, D., Ueki, K., Harsh, G. R. T., von Deimling, A., Gusella, J. F., Mohrenweiser, H. W., and Louis, D. N. Chromosome 19q deletions in human gliomas overlap telomeric to *D19S219* and may target a 425 kb region centromeric to *D19S112*. J. Neuropathol. Exp. Neurol., *54:* 622–626, 1995.
21. Ueki, K., Ramaswamy, S., Billings, S. J., Mohrenweiser, H. W., and Louis, D. N. ANOVA, a putative astrocytic RNA-binding protein gene that maps to chromosome 19q13.3. Neurogenetics, *1:* 31–36, 1997.
22. Yong, W. H., Ueki, K., Chou, D., Reeves, S. A., von Deimling, A., Gusella, J. F., Mohrenweiser, H. W., Buckler, A. J., and Louis, D. N. Cloning of a highly conserved human protein serine-threonine phosphatase gene from the glioma candidate region on chromosome 19q13.3. Genomics, *29:* 533–536, 1995.
23. Tikoo, A., Czekay, S., Viars, C., White, S., Heath, J. K., Arden, K., and Maruta, H. *p190-A*, a human tumor suppressor gene, maps to the chromosomal region 19q13.3 that is reportedly deleted in some gliomas. Gene (Amst.), *257:* 23–31, 2000.
24. Settleman, J., Narasimhan, V., Foster, L. C., and Weinberg, R. A. Molecular cloning of cDNAs encoding the GAP-associated protein p190: implications for a signaling pathway from ras to the nucleus. Cell, *69:* 539–549, 1992.
25. Lander, E. S., Linton, L. M., Birren, B., Nusbaum, C., Zody, M. C., Baldwin, J., Devon, K., Dewar, K., Doyle, M., FitzHugh, W., *et al.* Initial sequencing and analysis of the human genome. Nature (Lond.), *409:* 860–921, 2001.
26. Bruni, R., Fineschi, B., Ogle, W. O., and Roizman, B. A novel cellular protein, p60, interacting with both herpes simplex virus 1 regulatory proteins ICP22 and ICP0 is modified in a cell-type-specific manner and is recruited to the nucleus after infection. J. Virol., *73:* 3810–3817, 1999.
27. Saalmann, A., Munz, S., Ellerbrock, K., Ivell, R., and Kirchhoff, C. Novel sperm-binding proteins of epididymal origin contain four fibronectin type II-modules. Mol. Reprod. Dev., *58:* 88–100, 2001.
28. Haeseleer, F., Sokal, I., Verlinde, C. L., Erdjument-Bromage, H., Tempst, P., Pronin, A. N., Benovic, J. L., Fariss, R. N., and Palczewski, K. Five members of a novel Ca(2+)-binding protein (CABP) subfamily with similarity to calmodulin. J. Biol. Chem., *275:* 1247–1260, 2000.
29. Dowler, S., Currie, R. A., Campbell, D. G., Deak, M., Kular, G., Downes, C. P., and Alessi, D. R. Identification of pleckstrin-homology-domain-containing proteins with novel phosphoinositide-binding specificities. Biochem. J., *351:* 19–31, 2000.
30. Chou, D., Miyashita, T., Mohrenweiser, H. W., Ueki, K., Kastury, K., Druck, T., von Deimling, A., Huebner, K., Reed, J. C., and Louis, D. N. The *BAX* gene maps to the glioma candidate region at 19q13.3, but is not altered in human gliomas. Cancer Genet. Cytogenet., *88:* 136–140, 1996.
31. Venter, J. C., Adams, M. D., Myers, E. W., Li, P. W., Mural, R. J., Sutton, G. G., Smith, H. O., Yandell, M., Evans, C. A., Holt, R. A., *et al.* The sequence of the human genome. Science (Wash. DC), *291:* 1304–1351, 2001.
32. Wolfsberg, T. G., and Landsman, D. A comparison of expressed sequence tags (ESTs) to human genomic sequences. Nucleic Acids Res., *25:* 1626–1632, 1997.
33. Hillier, L. D., Lennon, G., Becker, M., Bonaldo, M. F., Chiapelli, B., Chissoe, S., Dietrich, N., DuBuque, T., Favello, A., Gish, W., Hawkins, M., Hultman, M., Kucaba, T., Lacy, M., Le, M., Le, N., Mardis, E., Moore, B., Morris, M., Parsons, J., Prange, C., Rifkin, L., Rohlfing, T., Schellenberg, K., Marra, M., *et al.* Generation and analysis of 280,000 human expressed sequence tags. Genome Res., *6:* 807–828, 1996.
34. Trofatter, J. A., MacCollin, M. M., Rutter, J. L., Murrell, J. R., Duyao, M. P., Parry, D. M., Eldridge, R., Kley, N., Menon, A. G., Pulaski, K., *et al.* A novel moesin-, ezrin-, radixin-like gene is a candidate for the neurofibromatosis 2 tumor suppressor. Cell, *72:* 791–800, 1993.
35. Yang, Y., Hwang, C. K., D'Souza, U. M., Lee, S. H., Junn, E., and Mouradian, M. M. Three-amino acid extension loop homeodomain proteins Meis2 and TGIF differentially regulate transcription. J. Biol. Chem., *275:* 20734–20741, 2000.
36. Imoto, I., Pimkhaokham, A., Watanabe, T., Saito-Ohara, F., Soeda, E., and Inazawa, J. Amplification and overexpression of *TGIF2*, a novel homeobox gene of the TALE superclass, in ovarian cancer cell lines. Biochem. Biophys. Res. Commun., *276:* 264–270, 2000.
37. Endo, K., Oki, E., Biedermann, V., Kojima, H., Yoshida, K., Johannes, F. J., Kufe, D., and Datta, R. Proteolytic cleavage and activation of protein kinase Cμ by caspase-3 in the apoptotic response of cells to 1-β-D-arabinofuranosylcytosine and other genotoxic agents. J. Biol. Chem., *275:* 18476–18481, 2000.
38. Sturany, S., Van Lint, J., Muller, F., Wilda, M., Hameister, H., Hocker, M., Brey, A., Gern, U., Vandenheede, J., Gress, T., Adler, G., and Seufferlein, T. Molecular cloning and characterization of the human protein kinase D2. A novel member of the protein kinase D family of serine threonine kinases. J. Biol. Chem., *276:* 3310–3318, 2001.
39. Wang, D. Z., Nur, E. K. M. S., Tikoo, A., Montague, W., and Maruta, H. The GTPase and Rho GAP domains of p190, a tumor suppressor protein that binds the M_r 120,000 Ras GAP, independently function as anti-Ras tumor suppressors. Cancer Res., *57:* 2478–2484, 1997.
40. Nakano, K., and Wousden, K. H. *PUMA*, a novel proapoptotic gene, is induced by p53. Mol. Cell, *7:* 683–694, 2001.
41. Yu, J., Zhang, L., Hwang, P. M., Kinzler, K. W., and Vogelstein, B. PUMA induces the rapid apoptosis of colorectal cancer cells. Mol. Cell, *7:* 673–682, 2001.
42. Moskow, J. J., Bullrich, F., Huebner, K., Daar, I. O., and Buchberg, A. M. Meis1, a *PBX1*-related homeobox gene involved in myeloid leukemia in BXH-2 mice. Mol. Cell. Biol., *15:* 5434–5443, 1995.
43. Kroon, E., Krosl, J., Thorsteinsdottir, U., Baban, S., Buchberg, A. M., and Sauvageau, G. Hoxa9 transforms primary bone marrow cells through specific collaboration with Meis1a but not Pbx1b. EMBO J., *17:* 3714–3725, 1998.
44. Pathan, N., Marusawa, H., Krajewska, M., Matsuzawa, S., Kim, H., Okada, K., Torii, S., Kitada, S., Krajewski, S., Welsh, K., Pio, F., Godzik, A., and Reed, J. C. TUCAN, an antiapoptotic caspase-associated recruitment domain family protein overexpressed in cancer. J. Biol. Chem., *276:* 32220–32229, 2001.
45. Bouchier-Hayes, L., Conroy, H., Egan, H., Adrain, C., Creagh, E. M., MacFarlane, M., and Martin, S. J. CARDINAL, a novel caspase recruitment domain protein, is an inhibitor of multiple NF-κB activation pathways. J. Biol. Chem., *76:* 44069–44077, 2001.
46. Qian, Y. W., Wang, Y. C., Hollingsworth, R. E., Jr., Jones, D., Ling, N., and Lee, E. Y. A retinoblastoma-binding protein related to a negative regulator of Ras in yeast. Nature (Lond.), *364:* 648–652, 1993.
47. Gaozza, E., Baker, S. J., Vora, R. K., and Reddy, E. P. AATYK: a novel tyrosine kinase induced during growth arrest and apoptosis of myeloid cells. Oncogene, *15:* 3127–3135, 1997.
48. Raghunath, M., Patti, R., Bannerman, P., Lee, C. M., Baker, S., Sutton, L. N., Phillips, P. C., and Damodar Reddy, C. A novel kinase, AATYK induces and promotes neuronal differentiation in a human neuroblastoma (SH-SY5Y) cell line. Brain Res. Mol. Brain Res., *77:* 151–162, 2000.
49. Serra-Pages, C., Medley, Q. G., Tang, M., Hart, A., and Streuli, M. Liprins, a family of LAR transmembrane protein-tyrosine phosphatase-interacting proteins. J. Biol. Chem., *273:* 15611–15620, 1998.
50. Devilee, P., Cleton-Jansen, A., and Cornelisse, C. J. Ever since Knudson. Trends Genet., *17:* 569–573, 2001.

Transcript Map of the 3.7-Mb *D19S112*–*D19S246* Candidate Tumor Suppressor Region on the Long Arm of Chromosome 19

Christian Hartmann, Loki Johnk, Gaspar Kitange, et al.

Cancer Res 2002;62:4100-4108.